Neurosci. Bull. November, 2022, 38(11):1347–1364
https://doi.org/10.1007/s12264-022-00914-w

www.neurosci.cn
www.springer.com/12264

ORIGINAL ARTICLE

Anti-Seizure and Neuronal Protective Effects of Irisin in Kainic Acid-Induced Chronic Epilepsy Model with Spontaneous Seizures

Jie Yu[1] · Yao Cheng[1] · Yaru Cui[1] · Yujie Zhai[1] · Wenshen Zhang[2] · Mengdi Zhang[1] · Wenyu Xin[1] · Jia Liang[1] · Xiaohong Pan[1] · Qiaoyun Wang[1] · Hongliu Sun[1]

Received: 26 August 2021 / Accepted: 19 April 2022 / Published online: 12 July 2022

Abstract An increased level of reactive oxygen species is a key factor in neuronal apoptosis and epileptic seizures. Irisin reportedly attenuates the apoptosis and injury induced by oxidative stress. Therefore, we evaluated the effects of exogenous irisin in a kainic acid (KA)-induced chronic spontaneous epilepsy rat model. The results indicated that exogenous irisin significantly attenuated the KA-induced neuronal injury, learning and memory defects, and seizures. Irisin treatment also increased the levels of brain-derived neurotrophic factor (BDNF) and uncoupling protein 2 (UCP2), which were initially reduced following KA administration. Furthermore, the specific inhibitor of UCP2 (genipin) was administered to evaluate the possible protective mechanism of irisin. The reduced apoptosis, neurodegeneration, and spontaneous seizures in rats treated with irisin were significantly reversed by genipin administration. Our findings indicated that neuronal injury in KA-induced chronic epilepsy might be related to reduced levels of BDNF and UCP2. Moreover, our results confirmed the inhibition of neuronal injury and epileptic seizures by exogenous irisin. The protective effects of irisin may be mediated through the BDNF-mediated UCP2 level. Our results thus highlight irisin as a valuable therapeutic strategy against neuronal injury and epileptic seizures.

Keywords Epilepsy · Seizure · Irisin · Genipin · Neuronal injury

Introduction

Epilepsy is a nervous system disorder that can induce persistent brain injury with serious pathological and psychological consequences [1, 2]. At present, ~50 million people suffer from epilepsy in the world, with an estimated 4–10 per thousand in the general population suffering from active epilepsy [3–5]. Epilepsy is a common chronic disease that affects people across different age groups [6, 7]. To date, the clinical management of epilepsy involves drug therapy, but drug resistance and adverse effects are critical issues that warrant attention [8, 9]. The limitations of drug-based therapy are closely related to the complex and unclear mechanisms underlying epilepsy. Further studies are warranted to better understand the mechanisms underlying the disease and to explore new and effective treatment options.

Increased production of reactive oxygen species (ROS) is an important mechanism in neuronal apoptosis and epileptic seizures [10, 11]. During a seizure, the increase of ROS results in the death of neurons and serious neurological damage [12, 13]. Furthermore, mitochondrial function has been shown to be closely associated with the production of ROS [14–16]. Mitochondria are the main site of ROS accumulation during a seizure and play a significant role in neuronal excitability [17]. Mitochondrial dysfunction and oxidative stress-induced injury are clear

Jie Yu, Yao Cheng, and Yaru Cui have contributed equally to this work.

Supplementary Information The online version contains supplementary material available at https://doi.org/10.1007/s12264-022-00914-w.

✉ Qiaoyun Wang
byylwqy@163.com

✉ Hongliu Sun
sun_china6@163.com; sunhongliu@bzmc.edu.cn

[1] School of Pharmaceutical Sciences, Binzhou Medical University, Yantai 264003, China

[2] The Sixth Scientific Research Department, Shandong Institute of Nonmetallic Materials, Jinan 250031, China

pathological changes in epilepsy [18]. Active oxygen production associated with mitochondrial dysfunction may affect the occurrence of epilepsy and inhibiting ROS can lead to attenuated seizures [19, 20].

Irisin has been confirmed to reduce the level of ROS as well as mitochondria-dependent apoptosis and injury caused by ischemia/reperfusion [21, 22]. Irisin is a glycosylated protein mainly secreted by skeletal muscle; its expression increases with exercise [23]. Within 30 min of rapid exercise, the irisin level increases in the circulation, which promotes glycolytic degradation and lipolysis in skeletal muscle [24]. Irisin is widely distributed across tissues, including the brain [25]. The cell-protective roles of irisin have garnered increasing attention over recent years [22, 26, 27]. According to Chen et al., irisin participates in mitochondrial biogenic functional activity and oxidative metabolism when the lung is injured by ischemia/reperfusion [21, 22]. Further, irisin reduces ROS production and mitochondria-dependent apoptosis, reducing the cellular injury caused by ischemia/reperfusion [21, 22]. In addition, Wang *et al*. [28] found that irisin reduces the area of cardiac infarction and improves heart function after ischemia by protecting mitochondrial function *via* the inhibition of both mitochondrial permeability transition pore opening and mitochondrial swelling [29]. Moreover, irisin can reduce apoptosis by decreasing the level of active caspase-3 and poly ADP-ribose polymerase, and by increasing the expression of superoxide dismutase and the phosphorylation of p38 [30].

Irisin is a type I membrane protein with 112 amino-acids and a molecular weight of 12 kDa [31]. It is formed after the hydrolyzation of fibronectin domain-containing protein 5 (FNDC5). Under the action of peroxisome proliferator-activated receptor γ coactivator 1α, FNDC5 is hydrolyzed in the amino-acid sites 30 and 142 to produce irisin [32, 33]. Exercise induces FNDC5 gene expression in skeletal muscle, thus increasing the concentration of irisin in the circulation [34, 35]. and it further induces brain-derived neurotrophic factor (BDNF) expression through the newly-produced irisin. Activation of the FNDC5/irisin/BDNF signaling pathway has been confirmed in the hippocampus through endurance exercise [34, 35]. BDNF is a neurotrophic factor primarily expressed in the central nervous system (CNS) [36, 37]; it promotes neuronal cell survival, differentiation, migration, dendrite growth, synaptogenesis, and synaptic plasticity [38]. Meanwhile, the level of BDNF is closely associated with epileptogenesis and seizures [39]. The expression of BDNF is significantly reduced in FNDC5$^{-/-}$ mice [21]. FNDC5 injection, without exercise, increases BDNF gene expression and promotes the growth and survival of brain neurons in mice [40]. Altogether, these results indicate a potential protective role of the FNDC5/irisin/BDNF pathway.

BDNF further promotes the expression of uncoupling proteins (UCPs) [41], which belong to the mitochondrial inner membrane protein family. The UCP family includes five members, which display different distributions and functions. UCP1 is expressed in brown adipose tissue and is responsible for heat production [42]. UCP2, which is expressed in the CNS [43], has been shown to have significant neuroprotective effects [43, 44]. UCP2 reduces mitochondria-mediated ROS production through uncoupling, increases ATP levels, reduces mitochondrial damage caused by free radicals, and helps neuronal cells to consume energy produced by cells and free radicals [45]. Elevated UCP2 levels reduce the seizure-induced death of excitotoxic cells and combat pathological changes in neurodegenerative disorders such as epilepsy and Alzheimer's disease [46]. Altogether, UCP2 emerges as a potentially important contributor to the protective effects regulated by BDNF.

We thus hypothesized that irisin may play neuro-protective and anti-epileptic roles by reducing oxidative stress through BDNF-mediated UCP2 levels. In this study, we investigated the expression of BDNF and UCP2, as well as the levels of oxidative stress and neuronal injury in kainic acid (KA)-induced epilepsy. Furthermore, exogenous irisin treatment and genipin (UCP2 inhibitor) treatment were administered to confirm the protective effects and possible mechanisms of irisin.

Materials and Methods

Animals and Surgery

Male Sprague-Dawley rats (8 weeks old; Pengyue Experimental Animal Center, No. SCXK 2017-0002, Jinan, China) weighing 280–310 g were used in experiments. The animals were allowed food and water ad libitum. All the experiments complied with the National Institutes of Health Guidelines for the Care and Use of Laboratory Animals (National Institutes of Health Publication No. 80-23, 1996 Revision) and with the Animal Ethics Regulations of the Experimental Animal Center of Binzhou Medical College (approval No. 2017003). All efforts were made to reduce the number of animals used and minimize pain to these animals.

The rats were anaesthetized with sodium pentobarbital (50 mg/kg, i.p.; CAS, 57-33-0, Xiya Reagent, China) and fixed in a stereotaxic apparatus (Anhui Zheng Hua Biological Instrument Equipment Co., Ltd., China). A stainless-steel cannula (RSD Life Science, China) was implanted into the left lateral ventricle [anteroposterior (AP): −1.0 mm; lateral (L): 1.8 mm; and ventral (V): −3.6 mm] and the hippocampal CA3 region (AP: −5.3 mm; L: −5 mm; V: −6 mm) of each rat. The recording electrode stripped of insulation (0.5 mm of each tip) was implanted into the right cortex

(AP: −3.2 mm; L: 3.0 mm; and V: −1.8 mm) for electroencephalogram (EEG) recording using the PowerLab system (AD Instruments, Sydney, NSW, Australia). The implanted electrode was connected to a microelectrode socket, which was bonded to the skull with dental cement (Shanghai Zhangjiang Biological Materials Co., Ltd., China). The rats recovered within 7 days after operation.

Drug Treatment and Seizure Recording

The KA-induced chronic epilepsy model with spontaneous seizures was used. KA (2 μg/μL, 1.33×10^{-3} mg/kg; CAS: 58002-62-3; Sigma, USA) was injected into the hippocampal CA3 region through the implanted cannula 7 days after operation. The rats in the control group were treated with saline instead of KA. In the Irisin+KA group, irisin (3 μg/μL and 50 μg/kg, Xingbao Biotechnology Co., Ltd, China) was delivered into the lateral ventricle 30 min before KA injection through the implanted cannula, and was injected once every three days up to day 15 according to previous studies [47, 48] and our pilot experiments. The Saline+KA group was treated with saline instead of irisin. To evaluate the effects of irisin and guarantee the rigor of our experiment, a control group and an irisin group were added (n = 10/group), and the method of irisin administration was as above.

Genipin (0.5 μg/μL and 8.25 μg/kg, CAS, 6902-77-8, Aladdin, China), the specific inhibitor of UCP2 [46], was delivered into the lateral ventricle 30 min before irisin administration (60 min before KA injection) through a stainless-steel cannula. Genipin and irisin were injected once every three days up to day 15, while the Saline+Irisin+KA group was treated with saline instead of genipin. The details of pharmacological administration are shown in Fig. S1. A total of 289 rats were used in this study, 5 rats in the Saline+KA group died due to severe seizures.

From day 30 after KA administration, spontaneous seizure behavior was observed, and EEGs were recorded for three consecutive days every 10 days, for example on days 30, 31, and 32, then days 40, 41, and 42…, until days 170, 171, and 172. Each rat was placed in a transparent resin observation box (50 cm × 30 cm) and recorded for three consecutive days at each observation time point. EEGs were digitized using filters (1 Hz low-pass and 50 Hz high-pass; PowerLab Biological Recording System, AD Instruments, Australia). The frequency spectrum and the power spectral density of EEGs were analyzed using the PowerLab Biological Recording System (AD Instruments). According to Racine's criteria [49], epileptic behavior was classified into stages 1 to 5. Stages 1–3 indicated focal seizures, with symptoms including squinting, continuous chewing, head-shaking, and unilateral forelimb lifting. Stages 4–5 indicated generalized seizures, including bilateral forelimb lifting, wet dog-like shaking, generalized convulsions, and prostration. An electroclinical seizure was defined as polyspike discharges >5 Hz, >2 times baseline EEG amplitude lasting >3 s [50].

Immunohistochemistry

As in our previous report [51], at the 24 h, and days 3, 15, and 170 time points after KA administration, 5 rats in each group were anesthetized with sodium pentobarbital (50 mg/kg, i.p.; CAS, 57-33-0, Xiya Reagent, China), perfused through the heart with 250 mL saline for 20–30 min until the liver became white, and then perfused with 250 mL of 4% paraformaldehyde. The brain was removed and immersed in 4% paraformaldehyde for 24 h followed by 30% sucrose. When the brain sank to the bottom, it was cut at ~2.3 mm to ~5 mm from posterior to the bregma (The Rat Brain in Stereotaxic Coordinates, Third Edition) into 12-μm sections on a cryomicrotome (CM1850, Leica, Germany). The sections were washed with 0.01 mol/L phosphate-buffered saline (PBS) and incubated at 37°C for 1 h with 10% bovine serum albumin. After blocking, 50 μL of the primary antibody mouse monoclonal anti-mouse BDNF (1:200, Abcam, ab205067) was added to each section, which were washed three times with 0.01 mol/L PBS and then kept overnight at 4°C. Fluorescein isothiocyanate goat anti-rabbit IgG (50 μL; FITC, 1:200, A0562, Beyotime, China) was added to each section, which were then incubated at 37 °C for 1 h. After three washes, 50 μL of DAPI (C1005, Beyotime, China) per section was added and the sections were incubated at 20 °C for 15 min. After washing with 0.01 mol/L PBS, each section was sealed with a coverslip. The fluorescence intensity of brain sub-regions was assessed by confocal microscopy (LSM 880, Zeiss, Germany). All samples were repeated three times and averaged under the same conditions. The images were observed and acquired at the same brightness level. Fluorescence intensity was analyzed using ImageJ 1.37 (National Institutes of Health, Bethesda, USA).

Fluoro-Jade B Staining

Fluoro-Jade B (FJB) is a fluorescein derivative dye that specifically binds to degenerating neurons [51–53]. Slides with adherent brain tissue were immersed in 1% NaOH/80% ethanol for 5 min and in 70% ethanol for 2 min [52, 53]. The following steps were followed: the slides were rinsed with distilled water for 2 min; wiped and immersed in 0.06% potassium permanganate for 15 min to maintain a constant background; and rinsed with distilled water for 2 min. A 0.0004% FJB staining solution was prepared with 4 mL of 0.01% FJB stock solution (AG310-30MG; Millipore, Burlington, MA, USA) and 96 mL of 0.1% glacial acetic acid. The slides were incubated in the 0.0004% FJB staining

solution for 20 min in the dark, rinsed with distilled water for 1 min, dried at 50°C for 10 min, cleared in xylene for 10 min, and sealed with neutral resin. The slides were observed under a fluorescence microscope (Olympus, IX73, Japan) with blue (450 nm) excitation light. FJB-positive signals were manually counted for analysis.

Oxidative Stress Detection

2',7'-dichlorofluorescin (DCF) level changes were measured in each group to assess the level of oxidative stress, as described in our previous studies [53, 54]. Briefly, after KA treatment, 5 rats in each group were sacrificed at two time points (24 h and 3 days) after anesthesia. The brains were quickly extracted, and the cortices and hippocampi were separated on ice, then filtered into single-cell suspensions with 0.01 mol/L PBS (10 μL/mg). 250 μL from each sample was added to 500 μL of DCF diacetate (10 μmol/L, Beyotime, S0033, China) and incubated at 37°C for 40 min without light [53]. Centrifugation was repeated to remove the supernatant and wash the cells. Using excitation at 488 nm and emission at 525 nm, fluorescence intensity was measured in each group using a fluorescence microplate reader (Thermo, USA) [52]. The DCF levels are presented as ratios relative to the values measured in the control group.

Evaluation of Mitochondrial Reactive Oxygen Species by Mito-SOX Fluorescence and Flow Cytometry

As in our previous studies [52, 53], following KA treatment, 5 rats from each group were sacrificed after anesthesia at 24 h and 3 days. Their brains were quickly extracted, and the cortices and hippocampi were separated. Mitochondrial ROS were detected using Mito-SOX™ (M36008, Thermo Fisher, USA). Similar to the method of DCF assessment, after immersion in 0.01 mol/L PBS, single-cell suspensions of cortices and hippocampi were separately prepared. 1 mL of 5 μmol/L Mito-SOX working solution was added to each cell suspension for incubation in the dark in a 37°C cell incubator for 10 min [54]. After washing, fluorescence intensity was measured at 510 nm excitation and 580 nm emission, using a fluorescence microplate reader (Thermo, USA) and flow cytometer (Becton, Dickinson and Co., USA).

Learning and Memory Tests

As previously described [54], the Morris water maze (ZS-001, Beijing Zhongshi Di Chuang Technology Development Co., Ltd, China) was used to evaluate the learning and memory of rats on day 170 after KA administration [55]. These experiments consisted of two parts: positioning navigation and spatial exploration [56]. Before the experiment, each rat was placed in the pool to swim freely for 2 min to familiarize with the environment. In the 4-day positioning navigation experiment, each rat was returned to the pool wall in any quadrant, and the time needed to find the platform was recorded. The space exploration experiment was carried out on day 5 [57]. The platform was removed, each rat was allowed to swim freely for 60 s, and the number of crossings was recorded. All rats performed the above tasks. The evaluation was latency to the platform, number of times through the platform, and time spent in the target quadrant and in the contralateral quadrant [58].

Simultaneously, the novel object recognition (NOR) test was applied at day 30 (n = 10/group). NOR is a common means of assessment of memory in rodent models such as rats [59]. This experiment was divided into three periods: adaptive, training, and testing periods [60]. The rats were handled gently daily for 2 days before the experiment in order to familiarize them to the testers [61]. In the habituation period, rats were allowed move freely for 10 min in the apparatus (50 cm × 60 cm × 60 cm box and no object was present). During the training period, two identical, firm and scentless objects A and B were placed equidistant away from the side walls. The rats were placed in the box equidistant from and facing away from the objects, and the duration of exploring the objects was recorded. After 14–16 h from the training session [62], object A was replaced with a new object C, which had a different color and shape from the previous two, and the rats were put in the box as in the training session. The duration of testing was 5 min. Finally, the learning and memory was evaluated by measuring the time spent on exploring the new object and by calculating the identification index (Identification index = Time exploring new object/Total time exploring both objects) [60]. The experimental environment was always quiet and kept at the same light intensity. Rats that were born with abnormal horizontal or vertical movements were excluded.

Western Blotting

For western blotting, the brain was micro-dissected into cortex and hippocampus on ice. After treatment with RIPA lysis buffer (Meilunbio, MA0151) and PMSF (Beyotime, ST506), 10 μL lysis buffer per mg of brain tissue was added. The tissue was then sonicated on ice and the protein concentration was determined using the BCA Protein Kit (P0012; Beyotime, China). The proteins from tissue samples were separated on 12% sodium dodecyl sulfate polyacrylamide gels and electrotransferred. After blocking with 5% skim milk for 3 h, the membranes were incubated with mouse monoclonal antibodies against BDNF (1:1000, ab205067, Abcam, UK), anti-rabbit UCP2 (1:2000, ab97931, Abcam, UK), anti-rabbit caspase-3 (1:1000, 9662, Cell Signaling Technology, USA), anti-rabbit activated caspase-3 (1:1000, ab2302, Abcam, UK), or glyceraldehyde-3-phosphate dehydrogenase (GAPDH, 1:1000, AB-P-R 001, Kangchen, China) at 4°C overnight. The bands

were incubated with horseradish peroxidase-conjugated IgG secondary antibodies. Images were acquired from different gels under the same electrophoresis conditions using an image analyzer (Odyssey, LI-COR Biosciences, USA). The results were the gray values of the target strips compared to the GAPDH band.

Statistical Analysis

The sample size was estimated based on our preliminary experiments and balanced one-way analysis of variance (ANOVA). All the data are shown as the mean ± SEM. Statistical analyses were carried out with SPSS 25.0 (IBM, USA). The cumulative number and duration in stages 1–3 between the Saline+KA and Irisin+KA groups were analyzed using the nonparametric Mann-Whitney U test. Cumulative seizure duration and latency to platform were analyzed by two-way ANOVA for repeated measures. The other parameters were analyzed by one-way ANOVA followed by a Dunnett's T3 *post-hoc* test. For all analyses, differences were considered significant at $P < 0.05$.

Results

Irisin Treatment has No Significant Toxic Side-effects

On day 30 after KA treatment, the heart, liver, spleen, lung, and kidney from rats treated with irisin were stained with hematoxylin-eosin (HE), and their weight and hair were assessed for 30 days ($n = 8$/group). Likewise, the novel object recognition test (day 30, $n = 10$/group), oxidative stress (24 h, $n = 5$/group), FJB staining (24 h, $n = 5$/group), and western blotting (24 h, $n = 5$/group) were also performed. The results of HE analogously showed no significant lesions in the organizational structure of the heart, liver, spleen, lung, and kidney (Fig. S4A), as well as no significant changes in body weight or hair color and texture due to irisin treatment (Fig. S4D). Meanwhile, the levels of caspase-3 increased slightly (cortex, $P = 0.041$; hippocampus, $P = 0.045$; Fig. S3A, B), accompanied by slightly decreased levels of activated caspase-3 (cortex, $P = 0.018$; hippocampus, $P = 0.033$; Fig. S3A, C), neuronal injury (CA2, $P = 0.032$; EC, $P = 0.025$; Fig. S3D, E), and oxidative stress (Fig. S3F, G) in irisin-treated rats compared to controls. Therefore, these results confirmed that no significant toxic side-effects occur after irisin treatment.

Exogenous Irisin Treatment Attenuates KA-induced Spontaneous Seizures

The spontaneous seizure behavior and EEGs were recorded in each group up to day 170 after KA treatment. In the Irisin+KA group ($n = 8$), the cumulative seizure duration was significantly shorter than that in the Saline+KA group ($n = 16$) at all time points from day 30 to day 170 ($P < 0.001$; Fig. 1A). Because the spontaneous seizures corresponded mainly to stages 1–3, the cumulative seizure number and the duration in these stages were further analyzed in each group. The results showed that irisin-treated rats had fewer seizures of shorter duration than rats treated with saline (Saline+KA; Fig. 1B, C). For example, on day 170, the cumulative duration (60.56 ± 3.36 s) and the number of stage 1–3 seizures (40.64 ± 3.86) in the Irisin+KA group were significantly lower than those in the Saline+KA group (359.30 ± 28.94 s, $P < 0.001$, Fig. 1B; 150.23 ± 17.70, $P < 0.001$; Fig. 1C). Representative EEGs and their power spectra analyses are presented in Fig. 1F–H. In addition, irisin treatment resulted in a longer latency of spontaneous seizures (Fig. 1E). Seizure and EEG results showed that exogenous irisin has a significant inhibitory effect on KA-induced chronic epileptic seizures. The detailed pharmacological manipulations and animal groups are presented in Fig.1D.

Effect of Irisin Treatment on the KA-induced Learning and Memory Defect

The differences in learning and memory after KA administration were evaluated with the water maze test. The results showed that the latency to reach the platform was significantly prolonged in KA-treated rats ($n = 12$) compared with control rats treated with saline ($n = 10$, $P < 0.001$, Fig. 2A). Moreover, KA-treated rats displayed a reduced target quadrant time ($P = 0.005$, Fig. 2B), longer opposite quadrant time ($P < 0.001$, Fig. 2C), and reduced target zone frequency ($P = 0.005$, Fig. 2D). Irisin treatment partly reversed the KA-induced learning and memory defect. In rats treated with irisin ($n = 8$), the latency to reach the platform ($P < 0.001$, Fig. 2A) and the time spent in the opposite quadrant ($P = 0.001$, Fig. 2C) were significantly shorter. Moreover, the time spent in the target quadrant ($P = 0.008$, Fig. 2B) and frequency of crossing the target zone ($P = 0.035$, Fig. 2D) significantly increased. Representative tracks of rats from each group searching for the platform are shown in Fig. 2E.

In addition, NOR testing showed that the identification index was lower in the Saline+KA group ($n = 10$; $P < 0.001$, Fig. 3K, L) than in controls. However, the rats had a higher identification index due to irisin administration ($n = 10$, Irisin+KA group; $P < 0.001$, Fig. 3L). Our results suggested that irisin treatment partly reverses the learning and memory impairment in KA-induced epilepsy.

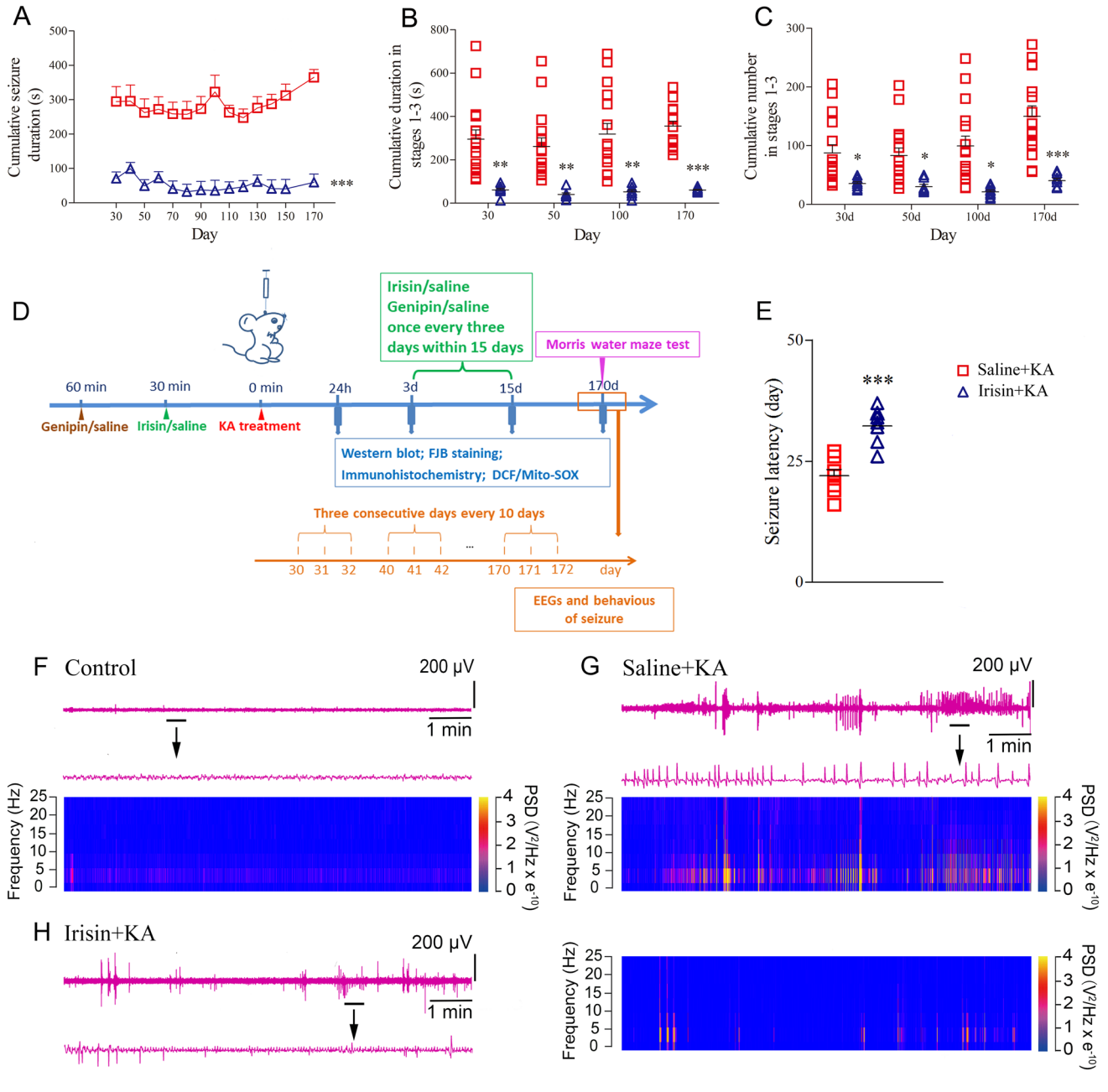

Fig. 1 Exogenous irisin treatment attenuates KA-induced spontaneous seizure severity and the learning and memory defect in rats. **A** Cumulative seizure duration of stage 1–5 seizures in each group from day 30 to day 170 following KA injection (Saline+KA group, $n = 16$; Irisin+KA group, $n = 8$). **B** Cumulative time of stage 1–3 seizures in each group. **C** Cumulative number of stage 1–3 seizures. **D** Schematic of the experimental design. **E** Latency of spontaneous seizures. **F–H** Representative electroencephalograms (EEGs) and corresponding analysis of frequency spectrum and power spectrum for each group on day 170. $^*P < 0.05$, $^{**}P < 0.01$, $^{***}P < 0.001$ *vs* Saline+KA group. KA, kainic acid.

Irisin Treatment Attenuates the Elevated Levels of Apoptosis and Neuronal Degeneration Induced by KA

Western blotting was used to analyze changes in the apoptosis-related proteins caspase-3 and activated caspase-3 on days 3 and 170 after KA administration ($n = 5$/group) to evaluate the effects of irisin on apoptosis. The results showed that KA administration significantly increased the level of activated caspase-3 in both cortex and hippocampus (day 3, cortex, $P < 0.001$; hippocampus, $P < 0.001$; Fig. 2F, I; day 170, cortex, $P < 0.001$; hippocampus, $P < 0.001$; Fig. 2G,

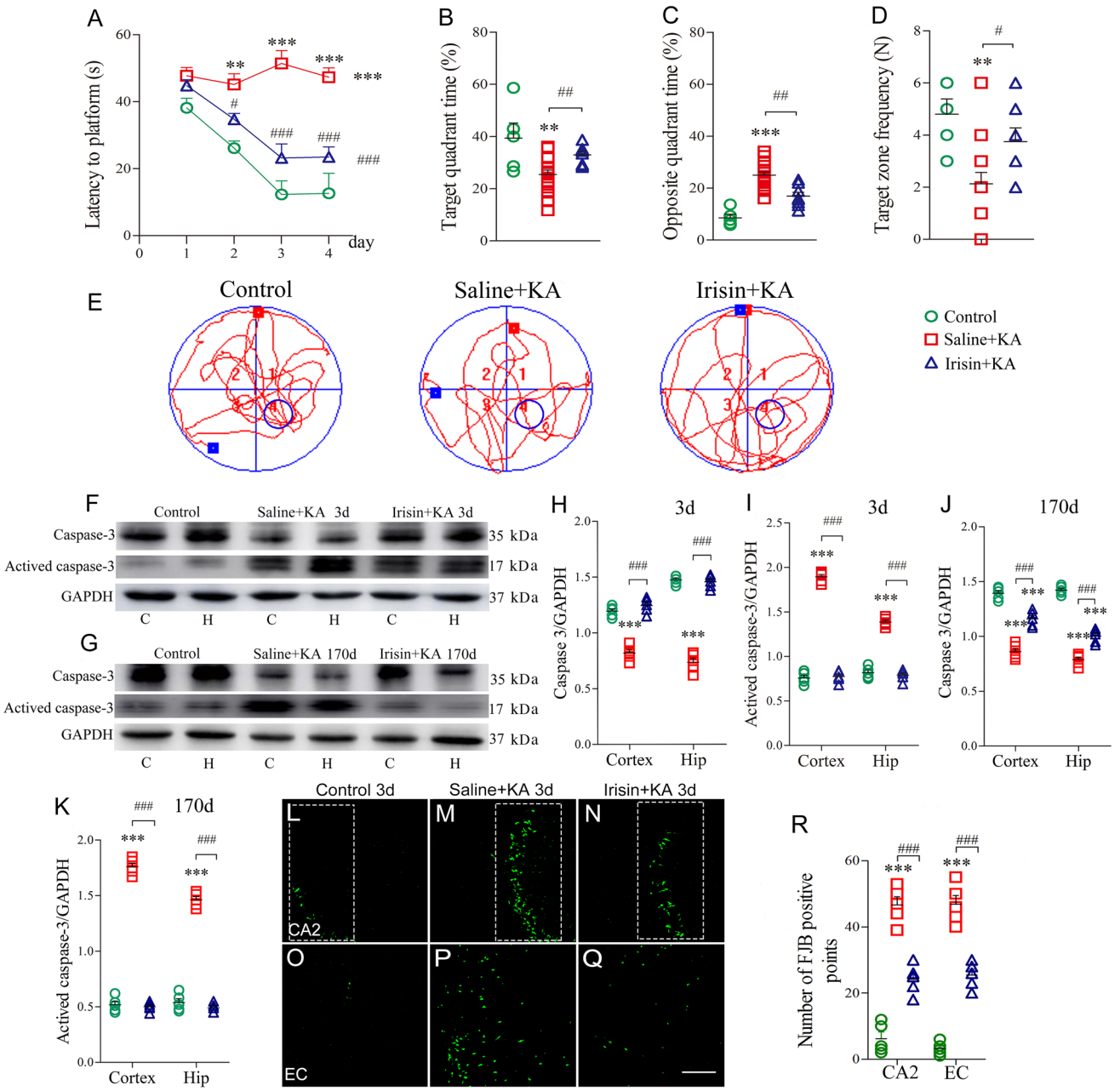

Fig. 2 Exogenous irisin treatment attenuates the elevated levels of apoptosis and neuronal degeneration induced by KA. **A** Latency to find platform (Control group, $n = 10$; Saline+KA group, $n = 16$; Irisin+KA group, $n = 8$). **B** Percentage of time in target quadrant. **C** Percentage of time in opposite quadrant. **D** Platform crossing times. **E** Trajectories in Morris water maze. **F, G** Immunoreactivity of caspase-3 and activated caspase-3 on days 3 and 170 after KA treatment ($n = 5$/group). **H–K** Normalized intensity of caspase-3 and activated caspase-3 relative to GAPDH. **L–R** FJB-positive signals in CA2 and EC ($n = 5$/group; scale bar, 50 μm) on day 3. $^{**}P < 0.01$, $^{***}P < 0.001$ *vs* control group; $^{\#}P < 0.05$, $^{\#\#}P < 0.01$, $^{\#\#\#}P < 0.001$ *vs* Saline+KA group (one-way ANOVA with Dunnett's T3 *post-hoc* test). KA, kainic acid; C, cortex; EC, entorhinal cortex; CA2, cornu ammonis 2; H/Hip, hippocampus; FJB, Fluoro-Jade B.

K), with a reduced caspase-3 level (Fig. 2F–H, J). However, the Irisin+KA group presented significantly lower levels of activated caspase-3 than those of the Saline+KA group (day 3, cortex, $P < 0.001$; hippocampus, $P < 0.001$; Fig. 2F, I; day 170, cortex, $P < 0.001$; hippocampus, $P < 0.001$; Fig. 2G, K). The results supported a strong anti-apoptosis effect of irisin on KA-induced apoptosis.

FJB staining was used to further analyze the degeneration of neurons ($n = 5$/group). FJB-positive signals in rats were counted 24 h and 3 days following KA administration.

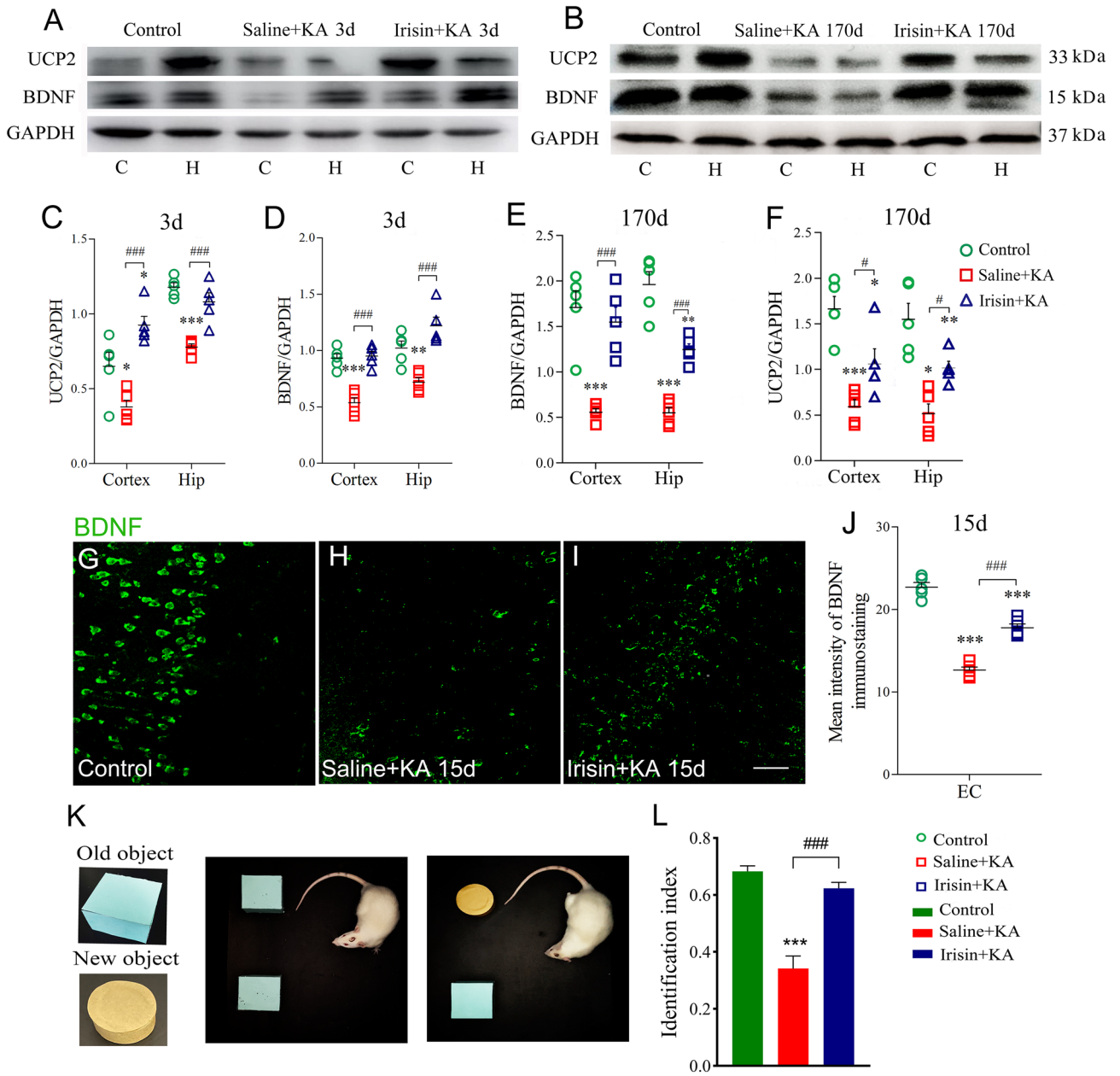

Fig. 3 Exogenous irisin treatment increases BDNF and UCP2 expression in cortex and hippocampus in KA-induced epilepsy. **A, B** Expression of UCP2 and BDNF on day 3 (**A**) and day 170 (**B**) after KA treatment (n = 5/group). **C–F** Normalized intensity of UCP2 and BDNF relative to GAPDH. **G–J** Mean fluorescence intensity of BDNF (green) (n = 5/group; scale bar, 30 μm). **K, L** The novel object recognition test (**K**) and the identification index (**L**) in each group (n = 10/group, on day 30). $^{*}P < 0.05$, $^{**}P < 0.01$, $^{***}P < 0.001$ *vs* controls; $^{\#}P < 0.05$, $^{\#\#\#}P < 0.001$ *vs* each other (one-way ANOVA with Dunnett's T3 *post-hoc* test). BDNF, brain-derived neurotrophic factor; UCP2, uncoupling protein 2; C, cortex; EC, entorhinal cortex; H/Hip, hippocampus; KA, kainic acid.

Significantly increased FJB-positive signals were observed in the hippocampus (CA2, $P < 0.001$, Fig. 2M, R) and entorhinal cortex (EC, $P < 0.001$, Fig. 2P, R) on day 3 after KA administration compared with those in the control group (Fig. 2L, O, R). Irisin treatment significantly reduced the number of FJB-positive signals in both the hippocampus ($P < 0.001$, Fig. 2N, R) and the EC ($P < 0.001$, Fig. 2Q, R) compared with those in the Saline+KA group. Similar changes in FJB signals were observed at 24 h (data not shown). The FJB staining results showed that KA induces significant neurodegeneration in the hippocampus and EC, and that irisin partly reverses this neuronal injury. Combined with the anti-apoptosis effects of irisin, the results showed a remarkable neuroprotective role of exogenous irisin treatment in KA-induced epilepsy.

Exogenous Irisin Treatment Increases BDNF and UCP2 Expression in the Hippocampus and Cortex in KA-Induced Epilepsy

The expression of BDNF and UCP2 in brain sub-regions was evaluated on days 3 and 170 in each group (n = 5/group). Western blotting showed decreased BDNF and UCP2 expression in the hippocampus and cortex on both day 3 (Fig. 3A, C, D) and day 170 (Fig. 3B, E, F) following KA administration. Immunohistochemistry also showed reduced levels of BDNF after KA administration (representative images in EC are shown in Fig. 3H, $P < 0.001$).

Exogenous irisin treatment significantly increased the level of BDNF as assessed by both western blotting (cortex and hippocampus, day 3, Fig. 3A, D; day 170, Fig. 3B, E) and immunohistochemistry (n = 5/group, EC, Fig. 3G–J) compared with the Saline+KA group. Synchronously, the elevated levels of UCP2 in the hippocampus and cortex were confirmed by western blots on both day 3 (Fig. 3A,C) and day 170 (Fig. 3B, F). Altogether, the results suggested that, in KA-induced chronic epilepsy, exogenous irisin treatment increases the expression of BDNF and UCP2 in the hippocampus and cortex.

Exogenous Irisin Treatment Reduces High KA-induced DCF/Mito-SOX Levels

The levels of oxidative stress were evaluated by measuring DCF/Mito-SOX [43] in the hippocampus and cortex 24 h and 3 days after KA administration (n = 5/group). KA administration led to a remarkable increase in the DCF level in both the cortex (Fig. 4A) and the hippocampus (Fig. 4B). Synchronously, the level of Mito-SOX was increased in the cortex (Fig. 4C) and the hippocampus (Fig. 4D) after KA administration. Conversely, in the Irisin+KA group, the DCF levels significantly decreased in the cortex (24 h, $P < 0.001$; day 3, $P < 0.001$, Fig. 4A) and in the hippocampus (24 h, $P < 0.001$; day 3, $P < 0.001$, Fig. 4B) compared with those in the Saline+KA group. Similarly, Mito-SOX showed decreased levels in rats treated with irisin in both the cortex (24 h, $P < 0.001$; day 3, $P < 0.001$, Fig. 4C) and the hippocampus (24 h, $P < 0.001$; day 3, $P < 0.001$, Fig. 4D). Representative Mito-SOX flow cytometry results for each group are shown in Fig. 4E. The results indicated that the increased levels of oxidative stress induced by KA are partly reversed by exogenous irisin treatment.

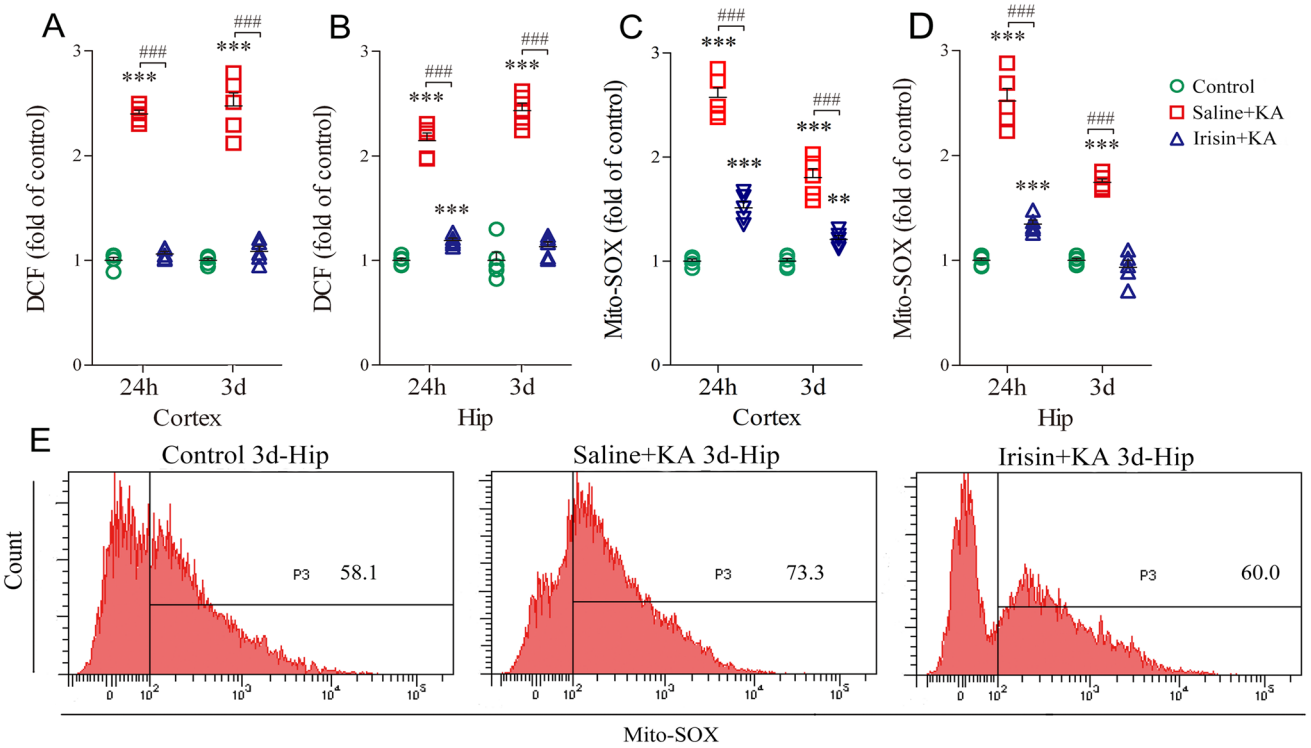

Fig. 4 Effects of exogenous irisin treatment on oxidative stress. **A, B** DCF levels in cortex and hippocampus (n = 5/group). **C, D** Mito-SOX levels in cortex and hippocampus (n = 5/group). **E** Representative Mito-SOX changes as measured by flow cytometry on day 3. $^{***}P < 0.001$ *vs* controls; $^{\#\#\#}P < 0.001$ *vs* each other (one-way ANOVA with Dunnett's T3 *post-hoc* test). Hip, hippocampus; KA, kainic acid; DCF, 2',7'-dichlorofluorescin.

Genipin Administration Reverses the Increased UCP2 and Reduced DCF and Mito-SOX Levels Due to Irisin Treatment

The expression of BDNF and UCP2 in brain sub-regions was measured in each group (n = 5/group) using western blotting on days 3 and 170 following KA administration. The results showed that their expression was significantly higher in irisin-treated rats (Saline+Irisin+KA) than in the Saline+KA group (Fig. 5A–F), while genipin administration (Genipin+Irisin+KA) decreased UCP2 expression in the hippocampus and cortex on both day 3 ($P < 0.001$, Fig. 5A, C) and day 170 ($P = 0.02$, cortex; $P = 0.03$, hippocampus, Fig. 5B, F) compared with the Saline+Irisin+KA group. However, the BDNF level showed almost no change after genipin treatment (Fig. 5A, B, D, E).

The levels of oxidative stress were assessed in the hippocampus and cortex at 24 h and 3 days after KA administration (n = 5/group). The results showed that genipin administration led to an increased level of DCF in both the cortex (24 h, $P < 0.001$; day 3, $P < 0.001$, Fig. 5G) and the hippocampus (24 h, $P < 0.001$; day 3, $P < 0.001$, Fig. 5H). Moreover, there was a similar increase in Mito-SOX levels in the cortex (Fig. 5I) and hippocampus (Fig. 5J) at 24 h and day 3 compared with those in the rats treated with saline (Saline+Irisin+KA group). Representative Mito-SOX flow cytometry results are shown in Fig. 5K. The results indicated that genipin reverses the reduction of oxidative stress by irisin as measured by DCF and Mito-SOX levels.

Genipin Administration Reverses the Attenuating Effect of Exogenous Irisin on KA-induced Epilepsy

Spontaneous seizure behavior and EEGs were recorded in each group at preset time points between days 30 and 170. In the Genipin+Irisin+KA group ($n = 10$), the cumulative seizure duration in stages 1–5 was significantly longer than that in the Saline+Irisin+KA group ($n = 8$) at all time points ($P < 0.001$, Fig. 6A). Because the spontaneous seizures mainly corresponded to stages 1–3, the cumulative number and the duration of stage 1–3 seizures were further analyzed in each group. The number and duration of seizures were greater in the genipin-treated rats than those in the Saline+Irisin+KA group (Fig. 6B, C). For example, at day 170, the cumulative duration (317.04 ± 50.14 s) and number (96.87 ± 19.11) of stages 1–3 seizures in the Genipin+Irisin+KA group were significantly higher than those in the Saline+Irisin+KA group (58.38 ± 5.78 s and 38.42 ± 8.64; $P < 0.001$, Fig. 6B, C). Representative EEGs and their power spectral analyses are shown in Fig. 6D–F. The behavioral and EEG results showed that genipin reverses the inhibition of KA-induced chronic epilepsy by exogenous irisin.

Genipin Administration Reverses the Irisin-mediated Enhancement of Learning and Memory in KA-induced Epilepsy

The differences in learning and memory were evaluated with the water maze test. The results showed that latency to reach the platform was significantly prolonged in genipin-treated rats ($n = 10$) compared with Saline+Irisin+KA rats ($n = 8$, $P < 0.001$, Fig. 6G). Moreover, there was a decrease in target quadrant time ($P = 0.002$, Fig. 6H) and target zone frequency ($P = 0.012$, Fig. 6J), together with a longer opposite quadrant time ($P < 0.001$, Fig. 6I). Meanwhile, the results of the NOR test showed that the elevated level of interaction with the new object in irisin-treated rats was reversed by genipin administration ($n = 10$, Genipin+Irisin+KA group, Fig. 7K, L). The results indicated that genipin partly reverses the protective effect of irisin against the learning and memory defect induced by KA. Representative tracks of rats searching for the platform are shown for each group in Fig. 6K.

Genipin Administration Reverses the Inhibitory Effect of Irisin on KA-induced Apoptosis and Neuronal Degeneration

Changes in the apoptosis-related proteins caspase-3 and activated caspase-3 were assessed by western blots on day 3 after KA administration to evaluate the effect of genipin on the anti-apoptosis effect of irisin. As described above, irisin significantly reduced the level of activated caspase-3 in both the cortex and hippocampus (day 3, cortex, $P < 0.001$; hippocampus, $P < 0.001$; Fig. 7A, C), with an increased caspase-3 level (Fig. 7A, B). The brain sub-regions of rats treated with genipin (Genipin+Irisin+KA group), however, showed a significantly higher level of activated caspase-3 than that in Saline+Irisin+KA rats (day 3, cortex, $P < 0.001$; hippocampus, $P < 0.001$; Fig. 7A, C). The results indicated that genipin reverses the anti-apoptosis effect of irisin on KA-induced apoptosis.

To analyze the degeneration of neurons further, FJB-positive signals were counted in each group of rats after KA administration (Fig. 7D–J). Significantly increased FJB-positive signals on day 3 were observed in both the hippocampus (CA2, $P < 0.001$, Fig. 7F, J) and EC ($P < 0.001$, Fig. 7I, J) in the Genipin+Irisin+KA group compared with those in the Saline+Irisin+KA group (CA2, Fig. 7E, J; EC, Fig. 7H, J). Similar changes in FJB signals were observed at 24 h (data not shown). The FJB staining results showed that the irisin-mediated inhibition of neuronal injury is reversed after genipin treatment. The results highlighted the potential contribution of UCP2 to the strong neuroprotective effect of irisin treatment in KA-induced epilepsy.

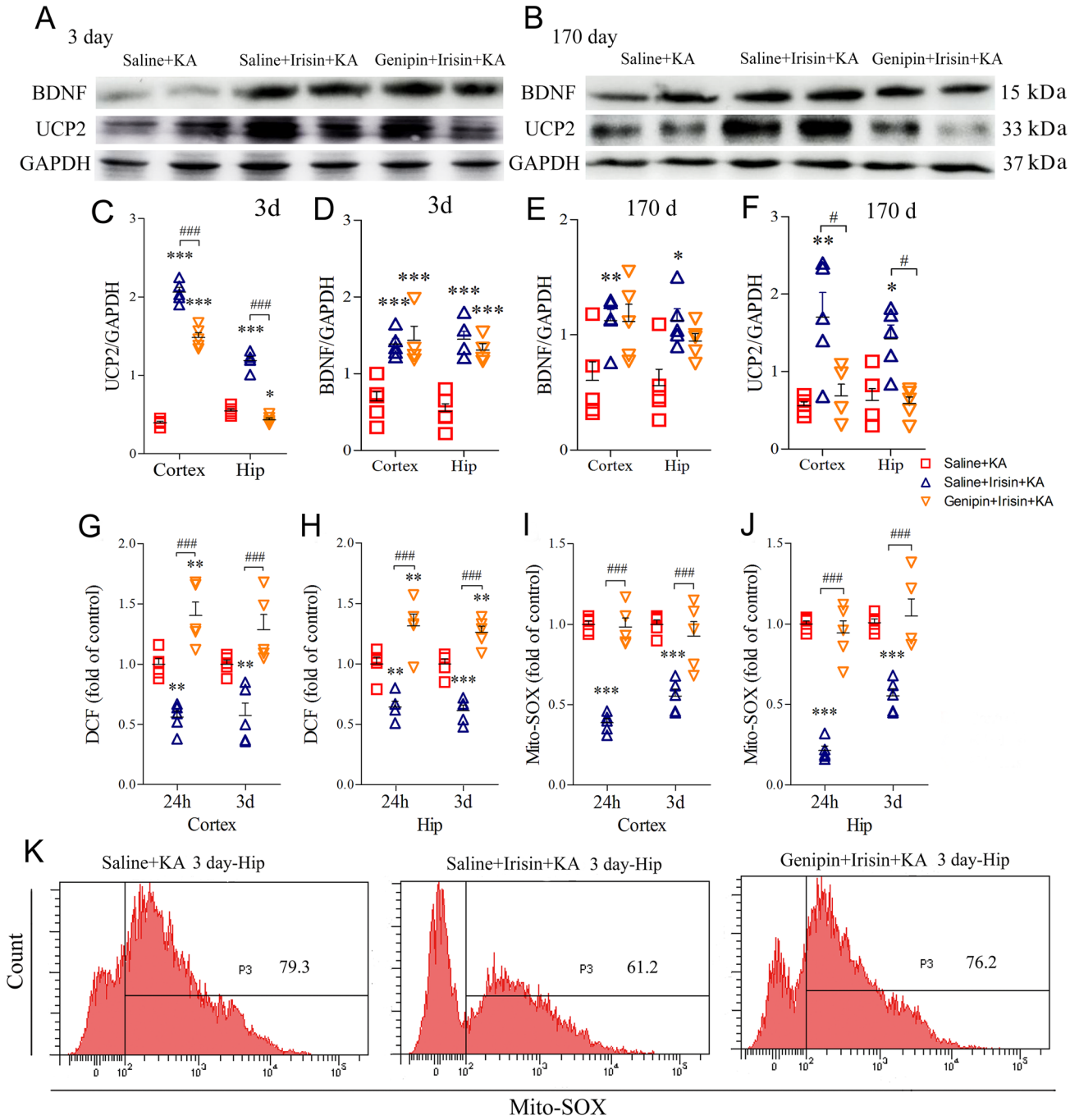

Fig. 5 Genipin administration reverses the increased level of UCP2 and oxidative stress reduction due to exogenous irisin treatment. **A, B** Levels of UCP2 and BDNF on day 3 (**A**) and day 170 (**B**) after KA treatment (n = 5/group). **C, F** Normalized intensity of UCP2 relative to GAPDH. **D, E** Normalized intensity of BDNF relative to GAPDH. **G, H** DCF levels in cortex and hippocampus (n = 5/group). **I, J** Mito-SOX levels in cortex and hippocampus (n = 5/group). **K** Representative Mito-SOX changes assessed by flow cytometry on day 3. $^{*}P < 0.05$, $^{**}P < 0.01$, $^{***}P < 0.001$ *vs* Saline+KA group; $^{\#}P < 0.05$, $^{\#\#\#}P < 0.001$ *vs* each other (one-way ANOVA with Dunnett's T3 *post-hoc* test). C, cortex; H/Hip, hippocampus; KA, kainic acid; BDNF, brain-derived neurotrophic factor; UCP2, uncoupling protein 2; DCF, 2',7'-dichlorofluorescin.

Discussion

Irisin is mainly produced in skeletal muscle after exercise [35]. During exercise, the expression of FNDC5/irisin in the CNS increases, in turn affecting a range of biological activities including mitochondrial biosynthesis, synaptic plasticity, mitochondrial Ca^{2+} homeostasis, and active oxygen generation [63, 64]. The above effects are closely associated

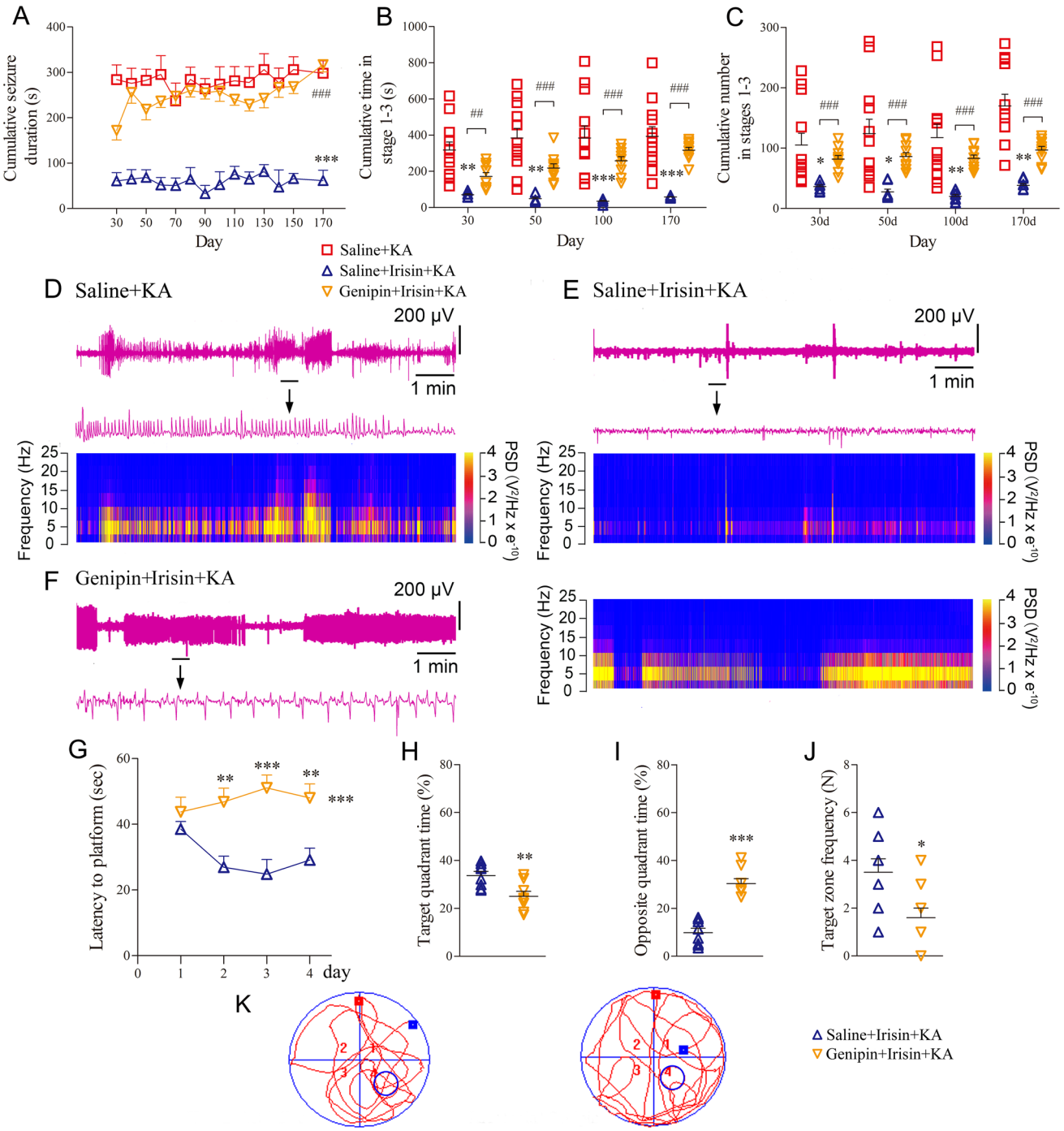

Fig. 6 Genipin administration reverses the protective effect of irisin administration on seizures and the learning and memory defect. **A** Cumulative seizure duration of stage 1–5 seizures from day 30 to day 170 after KA injection (Saline+KA group, n = 12; Irisin+KA group, n = 8; Genipin+Irisin+KA group, n = 10). **B** Cumulative time in stage 1–3 seizures. **C** Cumulative number of stage 1–3 seizures. **D–F** Representative electroencephalogram (EEGs) and corresponding analysis of frequency spectrum and power spectrum on day 170. $^{*}P < 0.05$, $^{**}P < 0.01$, $^{***}P < 0.001$ *vs* Saline+KA group (one-way ANOVA). $^{\#\#}P < 0.01$, $^{\#\#\#}P < 0.001$ *vs* each other (one-way ANOVA with Dunnett's T3 *post-hoc* test). **G** Latency to find the platform (Saline+Irisin+KA group, n = 8; Genipin+Irisin+KA group, n = 10). **H** Percentage of time in target quadrant. **I** Percentage of time in opposite quadrant. **J** Number of platform crossings. **K** Trajectories in Morris water maze. $^{*}P < 0.05$, $^{**}P < 0.01$, $^{***}P < 0.001$ *vs* Saline+Irisin+KA group (one-way ANOVA). KA, kainic acid.

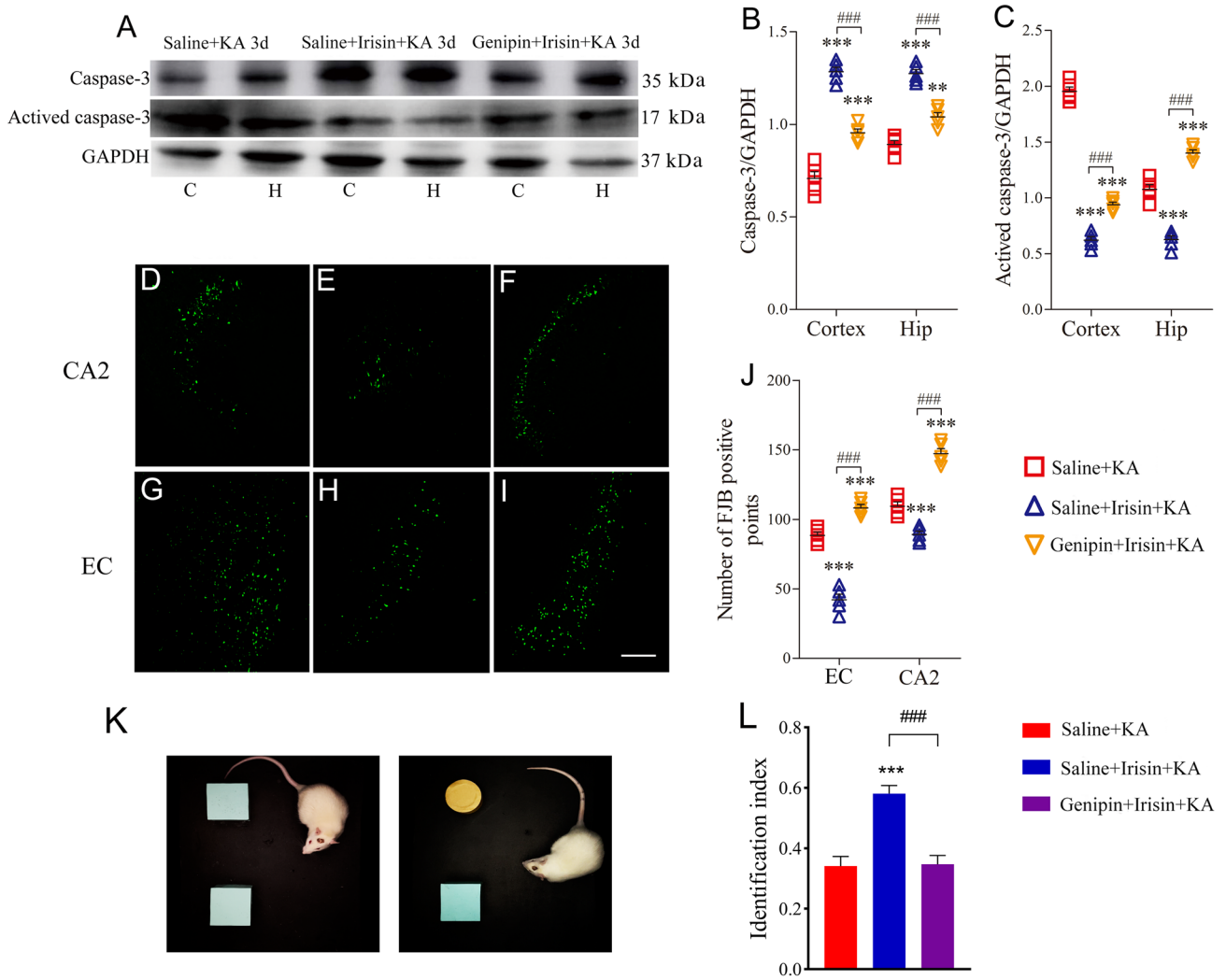

Fig. 7 Genipin reverses neuronal protection of exogenous irisin. **A–C** Levels of apoptosis-related proteins on day 3 (n = 5/group). **D–J** FJB (Fluoro-Jade B) signal patterns in CA2 and EC on day 3 (n = 5/group; scale bar, 100 μm). **K, L** The novel object recognition test (**K**) and identification index (**L**) of rats in each group (n = 10/group, on day 30). $^{**}P < 0.01$, $^{***}P < 0.001$ *vs* Saline+KA group (one-way ANOVA); $^{\#\#\#}P < 0.001$ *vs* each other (one-way ANOVA with Dunnett's T3 *post-hoc* test). C, cortex; CA2, cornu ammonis 2; EC, entorhinal cortex; H/Hip, hippocampus; KA, kainic acid.

with epileptogenesis and seizures [65–67]. For example, ROS-induced oxidative stress injuries have been found along with epilepsy and seizures [68, 69]. Mitochondria are vulnerable to oxidative stress and ROS-induced mitochondrial injury leads to defects in energy metabolism, which play key roles in the initiation and development of epilepsy [18]. Irisin has been shown to reduce oxidative stress damage and increase free radical scavenging in various models [70, 71]. For example, irisin significantly reduces the excessive accumulation of the superoxide anion and the production of malondialdehyde (the final oxidation product of lipid peroxidation) after cerebral tissue infarction due to ischemic injury [72]. Intravenous administration of exogenous irisin protects the heart from ischemia-reperfusion injury by increasing the expression of superoxide dismutase-1 and protecting mitochondrial function [29, 48]. Combined with the inhibitory effect of irisin on ROS production, the previous results led us to speculate that irisin might have a neuroprotective effect against epilepsy by reducing oxidative stress [73]. The results of our study confirmed our hypothesis. In the KA-induced chronic epilepsy model, irisin significantly attenuated the seizures and the learning and memory defect, as well as reducing neuronal injury and oxidative stress.

Interestingly, as irisin is mainly produced in skeletal muscle after exercise [35], over-excitation-induced contraction of skeletal muscle during the KA-induced seizures might lead to the increased irisin level. Indeed, an elevated irisin level has been reported in children with uncontrolled

epileptic seizures [74]. However, significant neuronal injury was found after KA administration. The results suggest that even if irisin might be produced by KA-induced seizures, it is not sufficient to resist the neuronal injury induced by KA administration. The detailed changes of endogenous irisin levels and the contribution in KA-induced chronic spontaneous epilepsy need further investigation.

The neuronal protection of irisin/FNDC5 through the regulation of BDNF has been confirmed. After endurance exercise, the level of FNDC5/irisin in the CNS is increased, further increasing the expression of BDNF in the brain [35]. Exogenous administration of irisin through the lateral ventricle leads to enhanced BDNF expression and reduced brain injury caused by ischemia-reperfusion [75]. Similarly, after intravenous injection of FNDC5, BDNF gene expression is increased in mouse cortical cell cultures and the hippocampus [35]. As the precursor of irisin, FNDC5 may regulate the expression of BDNF through hydrolyzing into irisin. As a neurotrophic factor, BDNF is closely associated with changes in cell survival and function [76], and epileptogenesis and seizures. Continuous release of BDNF in the epileptic hippocampus attenuates seizures, improves cognitive abilities, and reverses the histological and pathological changes in chronic epilepsy. In animal models of epilepsy induced by KA or pilocarpine, exogenous administration of BDNF reduces the toxic damage to neurons in the hippocampus [40]. Our results confirmed that exogenous irisin increased the expression of BDNF and significantly attenuated neuronal injury and seizure severity in KA-induced epilepsy, but there were almost no changes in the BDNF level with genipin pretreatment. These results indicated that irisin exerts its neuroprotective and anti-epileptic effects through the BDNF pathway.

However, there are two aspects of BDNF in epilepsy. According to previous studies, BDNF is closely associated with the growth of both normal and injured neurons and affects neurotransmitter synthesis and neuronal excitability [38, 77]. It has been reported that sharply elevated levels of BDNF could lead to temporal lobe epilepsy by activating tropomyosin receptor kinase B (TrκB) as well as other downstream signaling cascades [78, 79]. At the beginning of certain eclamptic events such as lesions and inflammation, the increased level of BDNF–TrκB in different regions of the brain may cause increased excitability of the limbic system [80]. Therefore, it was thought that high levels of this neurotrophin might promote epileptogenesis in epileptic or injured brains because it may participate in the establishment of an excitatory neural network (especially in the hippocampal region) during the latent period [79].

Nevertheless, some studies have reported that the elevated level of BDNF is one of the endogenous protective mechanisms in epilepsy: the increased expression of BDNF during a seizure protects neurons from further injury [81], and the upregulated levels of BDNF within the normal range decrease neuronal excitability by combining with the TrkB receptor [82, 83]. Accordingly, a previous statistical analysis reported that the level of BDNF in normal human plasma is 4289 ± 1810 pg/mL, which is significantly higher than that in the patients with epilepsy (977 ± 565 pg/mL) [84]. It has also been found that chronic injection of BDNF into the epileptic hippocampus reduces excitability, thus partly alleviating seizures [83]. Previous reports have suggested that the BDNF–TrκB pathway is an important factor in the occurrence of epilepsy and seizures, although the possible roles and mechanisms are controversial. Differences in BDNF levels and pathological states may explain its dual effects. More evidence is needed to establish the precise pathogenesis of BDNF–TrκB and its dual effects on epilepsy.

Downstream, the neuroprotective effect of BDNF is closely associated with UCP2, which has been shown to attenuate cell injury by inhibiting mitochondrial-mediated ROS production [66, 85, 86]. UCP2 is located in the inner membrane of the mitochondrion and belongs to a family of mitochondrial transporter proteins that are involved in energy production, apoptosis, and necrosis of cells [87]. In mitochondria, uncoupling of the respiratory chain and of oxidative phosphorylation converts the ADP of the proton gradient between the membrane space and the mitochondrial matrix into ATP. The energy destined to the ATP synthase disappears, it is consumed in the form of heat, and superoxide generation and energy storage are reduced [88]. The expression of mitochondrial UCP2 increases, followed by the uncoupling effect, and decreases cell death in animal models of acute brain injury [87] and Parkinson's disease [89]. Conversely, a decreased UCP2 level leads to a neurodegenerative process through mechanisms downstream from UCP2 [90, 91]. UCP2 stabilizes the mitochondrial inner membrane potential by changing the proton electrochemical concentration of the inner membrane, reduces the production of mitochondrial ROS and oxidative stress, and further protects myocardial cells from ischemia-reperfusion injury [85, 86]. Exogenous administration of BDNF upregulates UCP2 expression and reduces the nervous system damage caused by free radicals and oxidative stress [92]. As one of the BDNF regulators, exogenous irisin has also been reported to increase the expression of UCP2 [25]. Based on these results, we had reason to speculate that BDNF-regulated UCP2 might contribute to the anti-seizure and neuroprotective roles of irisin. Our results support this hypothesis. Increased expression of UCP2 and BDNF, and neuroprotective and anti-seizure effects were found after irisin treatment. Conversely, the UCP2 inhibitor genipin reversed the increase in UCP2 level, as well as attenuating the anti-seizure and neuroprotective effects of irisin.

Interestingly, irisin treatment 30 min before KA administration also attenuated the KA-induced acute seizures. The

results indicated an additional neuroprotective mechanism besides BDNF and UCP2 in the acute period, e.g. mitochondrial Ca^{2+} homeostasis and glutamate release [67]. Further, the less severe acute seizures may also contribute to the attenuated chronic spontaneous seizures. The detailed mechanisms need to be explored by further research.

The pathological hallmarks of epilepsy are neuronal apoptosis and brain injury, which are caused by epilepsy-induced excitotoxicity [93]. We used FJB staining to evaluate the neuronal damage caused by KA and the neuronal protection of irisin [54, 94]. The results showed that FJB-positive signals induced by KA were mainly located in the hippocampus and EC. Irisin reduced the FJB signals in the brain of epileptic rats. The hippocampus and EC are closely associated with seizures and cognition [95, 96]. Injury to the EC, which forms an epileptic network loop with the hippocampus, produces the recurrence of epileptic attacks, and further causes neuronal apoptosis [54, 96, 97]. Irisin can attenuate such neuronal damage [98]. Our experiments also showed that irisin protected against the neuroexcitatory damage in the hippocampus and EC induced by KA. Inhibiting the formation of the epileptic circuit by inhibiting neuronal damage in the hippocampus and EC may contribute to the anti-seizure effects of irisin, even though duality of the GABAergic signal on the excitability of neurons has been reported [28, 99].

In addition, in KA-induced chronic spontaneous epilepsy, increased levels of oxidative stress and neuronal injury were found as early as 24 h, which is much earlier than the occurrence of spontaneous seizures. The results indicated a possible contribution of early neuronal injury to the later seizures. Moreover, the early intervention in oxidative stress and neuronal injury by exogenous irisin treatment significantly attenuated the later spontaneous seizures. Consequently, the early neuropathy after epileptogenic stimulation may play a critical role in the subsequent epileptogenesis. The early protection against oxidative stress-induced neuronal injury may be a promising therapeutic strategy for epilepsy.

In conclusion, exogenous irisin treatment significantly increased the expression of BDNF and UCP2. Meanwhile, irisin treatment reduced oxidative stress, neuronal injury, learning and memory defects, and epileptic seizures. Administration of a UCP2 inhibitor confirmed the anti-seizure and neuroprotective effects of early irisin treatment in the KA-induced epilepsy model, and further indicated that the changed UCP2 level mediated by BDNF may be the underlying protective mechanism in this model.

Acknowledgements This work was supported by the National Natural Science Foundation of China (81573412 and 81803546), Key Research and Development Plan of Shandong Province (2018GSF121004), and Yantai Science and Technology Development Plan (2019xdhz098). We would like to thank Editage for English language editing.

Conflict of interest The authors claim that there are no conflicts of interest.

References

1. Wurina S, Zang YF, Zhao SG. Resting-state fMRI studies in epilepsy. Neurosci Bull 2012, 28: 449–455.
2. Liu YQ, Yu F, Liu WH, He XH, Peng BW. Dysfunction of hippocampal interneurons in epilepsy. Neurosci Bull 2014, 30: 985–998.
3. Mishra CB, Kumari S, Prakash A, Yadav R, Tiwari AK, Pandey P. Discovery of novel Methylsulfonyl phenyl derivatives as potent human Cyclooxygenase-2 inhibitors with effective anticonvulsant action: Design, synthesis, in-silico, *in-vitro* and *in-vivo* evaluation. Eur J Med Chem 2018, 151: 520–532.
4. Ngugi AK, Bottomley C, Fegan G, Chengo E, Odhiambo R, Bauni E, *et al*. Premature mortality in active convulsive epilepsy in rural Kenya: Causes and associated factors. Neurology 2014, 82: 582–589.
5. Eid T, Lee TSW, Patrylo P, Zaveri HP. Astrocytes and glutamine synthetase in epileptogenesis. J Neurosci Res 2019, 97: 1345–1362.
6. Jin MM, Chen Z. Role of gap junctions in epilepsy. Neurosci Bull 2011, 27: 389–406.
7. Qi YB, Cheng HM, Wang Y, Chen Z. Revealing the precise role of calretinin neurons in epilepsy: We are on the way. Neurosci Bull 2022, 38: 209–222.
8. Kharatishvili I, Nissinen JP, McIntosh TK, Pitkänen A. A model of posttraumatic epilepsy induced by lateral fluid-percussion brain injury in rats. Neuroscience 2006, 140: 685–697.
9. Wang Y, Chen Z. An update for epilepsy research and antiepileptic drug development: Toward precise circuit therapy. Pharmacol Ther 2019, 201: 77–93.
10. Lee KI, Lin JW, Su CC, Fang KM, Yang CY, Kuo CY, *et al*. Silica nanoparticles induce caspase-dependent apoptosis through reactive oxygen species-activated endoplasmic reticulum stress pathway in neuronal cells. Toxicol In Vitro 2020, 63: 104739.
11. Lichota A, Gwozdzinski L, Gwozdzinski K. Therapeutic potential of natural compounds in inflammation and chronic venous insufficiency. Eur J Med Chem 2019, 176: 68–91.
12. Smilin Bell Aseervatham G, Abbirami E, Sivasudha T, Ruckmani K. Passiflora caerulea L Fruit extract and its metabolites ameliorate epileptic seizure, cognitive deficit and oxidative stress in pilocarpine-induced epileptic mice. Metab Brain Dis 2020, 35: 159–173.
13. Xie NC, Wang C, Wu CJ, Cheng X, Gao YL, Zhang HF, *et al*. Mdivi-1 protects epileptic hippocampal neurons from apoptosis via inhibiting oxidative stress and endoplasmic reticulum stress *in vitro*. Neurochem Res 2016, 41: 1335–1342.
14. Li MM, Li X, Cao ZL, Wu YT, Chen J, Gao J, *et al*. Mitochondria-targeting BODIPY-loaded micelles as novel class of photosensitizer for photodynamic therapy. Eur J Med Chem 2018, 157: 599–609.
15. Pierce JD, Gupte R, Thimmesch A, Shen QH, Hiebert JB, Brooks WM, *et al*. Ubiquinol treatment for TBI in male rats: Effects on mitochondrial integrity, injury severity, and neurometabolism. J Neurosci Res 2018, 96: 1080–1092.
16. Wang C, Xie NC, Wang YL, Li YL, Ge XJ, Wang ML. Role of the mitochondrial calcium uniporter in rat hippocampal neuronal death after pilocarpine-induced status epilepticus. Neurochem Res 2015, 40: 1739–1746.
17. Waldbaum S, Patel M. Mitochondria, oxidative stress, and temporal lobe epilepsy. Epilepsy Res 2010, 88: 23–45.

18. Rowley S, Liang LP, Fulton R, Shimizu T, Day B, Patel M. Mitochondrial respiration deficits driven by reactive oxygen species in experimental temporal lobe epilepsy. Neurobiol Dis 2015, 75: 151–158.
19. Folbergrová J, Jesina P, Haugvicová R, Lisý V, Houstek J. Sustained deficiency of mitochondrial complex I activity during long periods of survival after seizures induced in immature rats by homocysteic acid. Neurochem Int 2010, 56: 394–403.
20. Folbergrová J, Ješina P, Kubová H, Otáhal J. Effect of resveratrol on oxidative stress and mitochondrial dysfunction in immature brain during epileptogenesis. Mol Neurobiol 2018, 55: 7512–7522.
21. Ng CSH, Wan S, Arifi AA, Yim APC. Inflammatory response to pulmonary ischemia-reperfusion injury. Surg Today 2006, 36: 205–214.
22. Chen K, Xu ZC, Liu YK, Wang Z, Li Y, Xu XF, *et al*. Irisin protects mitochondria function during pulmonary ischemia/reperfusion injury. Sci Transl Med 2017, 9: eaao6298.
23. Boström P, Wu J, Jedrychowski MP, Korde A, Ye L, Lo JC, *et al*. A PGC1-α-dependent myokine that drives brown-fat-like development of white fat and thermogenesis. Nature 2012, 481: 463–468.
24. Huh JY, Panagiotou G, Mougios V, Brinkoetter M, Vamvini MT, Schneider BE, *et al*. FNDC5 and irisin in humans: I. Predictors of circulating concentrations in serum and plasma and II. mRNA expression and circulating concentrations in response to weight loss and exercise. Metabolism 2012, 61: 1725–1738.
25. Erden Y, Tekin S, Sandal S, Onalan EE, Tektemur A, Kirbag S. Effects of central irisin administration on the uncoupling proteins in rat brain. Neurosci Lett 2016, 618: 6–13.
26. Zhang Y, Li R, Meng Y, Li SW, Donelan W, Zhao Y, *et al*. Irisin stimulates browning of white adipocytes through mitogen-activated protein kinase p38 MAP kinase and ERK MAP kinase signaling. Diabetes 2014, 63: 514–525.
27. Friedenreich CM, Neilson HK, Lynch BM. State of the epidemiological evidence on physical activity and cancer prevention. Eur J Cancer 2010, 46: 2593–2604.
28. Wang Y, Xu CL, Xu ZH, Ji CH, Liang J, Wang Y, *et al*. Depolarized GABAergic signaling in subicular microcircuits mediates generalized seizure in temporal lobe epilepsy. Neuron 2017, 95: 92-105.e5.
29. Wang H, Zhao YT, Zhang SY, Dubielecka PM, Du JF, Yano N, *et al*. Irisin plays a pivotal role to protect the heart against ischemia and reperfusion injury. J Cell Physiol 2017, 232: 3775–3785.
30. Wang Z, Chen K, Han Y, Zhu H, Zhou XY, Tan T, *et al*. Irisin protects heart against ischemia-reperfusion injury through a SOD2-dependent mitochondria mechanism. J Cardiovasc Pharmacol 2018, 72: 259–269.
31. Zhang WZ, Chang L, Zhang C, Zhang R, Li ZR, Chai BX, *et al*. Central and peripheral irisin differentially regulate blood pressure. Cardiovasc Drugs Ther 2015, 29: 121–127.
32. Abedpoor N, Taghian F, Ghaedi K, Niktab I, Safaeinejad Z, Rabiee F, *et al*. PPARγ/Pgc-1α-Fndc5 pathway up-regulation in gastrocnemius and heart muscle of exercised, branched chain amino acid diet fed mice. Nutr Metab (Lond) 2018, 15: 59.
33. Teufel A, Malik N, Mukhopadhyay M, Westphal H. Frcp1 and Frcp2, two novel fibronectin type III repeat containing genes. Gene 2002, 297: 79–83.
34. Wrann CD. FNDC5/irisin - their role in the nervous system and as a mediator for beneficial effects of exercise on the brain. Brain Plast 2015, 1: 55–61.
35. Wrann CD, White JP, Salogiannnis J, Laznik-Bogoslavski D, Wu J, Ma D, *et al*. Exercise induces hippocampal BDNF through a PGC-1α/FNDC5 pathway. Cell Metab 2013, 18: 649–659.
36. Dinda B, Dinda M, Kulsi G, Chakraborty A, Dinda S. Therapeutic potentials of plant iridoids in Alzheimer's and Parkinson's diseases: A review. Eur J Med Chem 2019, 169: 185–199.
37. Belviranli M, Okudan N, Kabak B, Erdoğan M, Karanfilci M. The relationship between brain-derived neurotrophic factor, irisin and cognitive skills of endurance athletes. Phys Sportsmed 2016, 44: 290–296.
38. Kuipers SD, Bramham CR. Brain-derived neurotrophic factor mechanisms and function in adult synaptic plasticity: New insights and implications for therapy. Curr Opin Drug Discov Devel 2006, 9: 580–586.
39. Xia DY, Huang X, Bi CF, Mao LL, Peng LJ, Qian HR. PGC-1α or FNDC5 is involved in modulating the effects of $A\beta_{1\text{-}42}$ oligomers on suppressing the expression of BDNF, a beneficial factor for inhibiting neuronal apoptosis, Aβ deposition and cognitive decline of APP/PS1 Tg mice. Front Aging Neurosci 2017, 9: 65.
40. Falcicchia C, Paolone G, Emerich DF, Lovisari F, Bell WJ, Fradet T, *et al*. Seizure-suppressant and neuroprotective effects of encapsulated BDNF-producing cells in a rat model of temporal lobe epilepsy. Mol Ther Methods Clin Dev 2018, 9: 211–224.
41. Wang CF, Bomberg E, Billington CJ, Levine AS, Kotz CM. Brain-derived neurotrophic factor (BDNF) in the hypothalamic ventromedial nucleus increases energy expenditure. Brain Res 2010, 1336: 66–77.
42. Bonet ML, Mercader J, Palou A. A nutritional perspective on UCP1-dependent thermogenesis. Biochimie 2017, 134: 99–117.
43. Hoang T, Smith MD, Jelokhani-Niaraki M. Toward understanding the mechanism of ion transport activity of neuronal uncoupling proteins UCP2, UCP4, and UCP5. Biochemistry 2012, 51: 4004–4014.
44. Binienda ZK, Ali SF, Virmani A, Amato A, Salem N, Przybyla BD. Co-regulation of dopamine D1 receptor and uncoupling protein-2 expression in 3-nitropropionic acid-induced neurotoxicity: Neuroprotective role of L-carnitine. Neurosci Lett 2006, 410: 62–65.
45. Diano S, Matthews RT, Patrylo P, Yang LC, Beal MF, Barnstable CJ, *et al*. Uncoupling protein 2 prevents neuronal death including that occurring during seizures: A mechanism for preconditioning. Endocrinology 2003, 144: 5014–5021.
46. Zhao BS, Sun LK, Jiang XR, Zhang Y, Kang JS, Meng H, *et al*. Genipin protects against cerebral ischemia-reperfusion injury by regulating the UCP2-SIRT3 signaling pathway. Eur J Pharmacol 2019, 845: 56–64.
47. Flori L, Testai L, Calderone V. The, "irisin system": From biological roles to pharmacological and nutraceutical perspectives. Life Sci 2021, 267: 118954.
48. Zhu D, Wang HC, Zhang JL, Zhang XT, Xin C, Zhang FY, *et al*. Irisin improves endothelial function in type 2 diabetes through reducing oxidative/nitrative stresses. J Mol Cell Cardiol 2015, 87: 138–147.
49. Ren YF, Qiu ML, Zhang J, Bi JB, Wang MZ, Hu LS, *et al*. Low serum irisin concentration is associated with poor outcomes in patients with acute pancreatitis, and irisin administration protects against experimental acute pancreatitis. Antioxid Redox Signal 2019, 31: 771–785.
50. Racine RJ. Modification of seizure activity by electrical stimulation. II. Motor seizure. Electroencephalogr Clin Neurophysiol 1972, 32: 281–294.
51. Liu T, Ma XR, Ouyang TX, Chen HP, Xiao Y, Huang YY, *et al*. Efficacy of 5-aminolevulinic acid-based photodynamic therapy against keloid compromised by downregulation of SIRT1-SIRT3-SOD2-mROS dependent autophagy pathway. Redox Biol 2019, 20: 195–203.
52. Zhang MD, Cui YR, Zhu W, Yu J, Cheng Y, Wu XD, *et al*. Attenuation of the mutual elevation of iron accumulation and oxidative stress may contribute to the neuroprotective and anti-seizure effects of xenon in neonatal hypoxia-induced seizures. Free Radic Biol Med 2020, 161: 212–223.

53. Zhang YR, Zhang MD, Zhu W, Yu J, Wang QY, Zhang JJ, *et al*. Succinate accumulation induces mitochondrial reactive oxygen species generation and promotes status epilepticus in the kainic acid rat model. Redox Biol 2020, 28: 101365.
54. Zhang YR, Zhang MD, Liu SH, Zhu W, Yu J, Cui YR, *et al*. Xenon exerts anti-seizure and neuroprotective effects in kainic acid-induced status epilepticus and neonatal hypoxia-induced seizure. Exp Neurol 2019, 322: 113054.
55. Morris R. Developments of a water-maze procedure for studying spatial learning in the rat. J Neurosci Methods 1984, 11: 47–60.
56. Vorhees CV, Williams MT. Morris water maze: Procedures for assessing spatial and related forms of learning and memory. Nat Protoc 2006, 1: 848–858.
57. Bromley-Brits K, Deng Y, Song W. Morris water maze test for learning and memory deficits in Alzheimer's disease model mice. J Vis Exp 2011: 2920.
58. Pereira LO, Arteni NS, Petersen RC, da Rocha AP, Achaval M, Netto CA. Effects of daily environmental enrichment on memory deficits and brain injury following neonatal hypoxia-ischemia in the rat. Neurobiol Learn Mem 2007, 87: 101–108.
59. Antunes M, Biala G. The novel object recognition memory: Neurobiology, test procedure, and its modifications. Cogn Process 2012, 13: 93–110.
60. Mathiasen JR, DiCamillo A. Novel object recognition in the rat: A facile assay for cognitive function. Curr Protoc Pharmacol 2010, Chapter 5: Unit5.59.
61. Lueptow LM. Novel object recognition test for the investigation of learning and memory in mice. J Vis Exp 2017, 126: 55718.
62. Zhang R, Xue GZ, Wang SD, Zhang LH, Shi CJ, Xie X. Novel object recognition as a facile behavior test for evaluating drug effects in AβPP/PS_1 Alzheimer's disease mouse model. J Alzheimers Dis 2012, 31: 801–812.
63. Andrews ZB, Horvath B, Barnstable CJ, Elsworth J, Yang LC, Beal MF, *et al*. Uncoupling protein-2 is critical for nigral dopamine cell survival in a mouse model of Parkinson's disease. J Neurosci 2005, 25: 184–191.
64. Echtay KS. Mitochondrial uncoupling proteins—what is their physiological role? Free Radic Biol Med 2007, 43: 1351–1371.
65. Vaynman S, Ying Z, Gómez-Pinilla F. Exercise induces BDNF and synapsin I to specific hippocampal subfields. J Neurosci Res 2004, 76: 356–362.
66. Migliaccio V, Scudiero R, Sica R, Lionetti L, Putti R. Oxidative stress and mitochondrial uncoupling protein 2 expression in hepatic steatosis induced by exposure to xenobiotic DDE and high fat diet in male Wistar rats. PLoS One 2019, 14: e0215955.
67. Bannai H, Niwa F, Sherwood MW, Shrivastava AN, Arizono M, Miyamoto A, *et al*. Bidirectional control of synaptic GABAAR clustering by glutamate and calcium. Cell Rep 2015, 13: 2768–2780.
68. Yang XY, Tse MCL, Hu X, Jia WH, Du GH, Chan CB. Interaction of CREB and PGC-1α induces fibronectin type III domain-containing protein 5 expression in C2C12 myotubes. Cell Physiol Biochem 2018, 50: 1574–1584.
69. Bhatti J, Nascimento B, Akhtar U, Rhind SG, Tien H, Nathens A, *et al*. Systematic review of human and animal studies examining the efficacy and safety of N-Acetylcysteine (NAC) and N-Acetylcysteine amide (NACA) in traumatic brain injury: Impact on neurofunctional outcome and biomarkers of oxidative stress and inflammation. Front Neurol 2017, 8: 744.
70. Askari H, Rajani SF, Poorebrahim M, Haghi-Aminjan H, Raeis-Abdollahi E, Abdollahi M. A glance at the therapeutic potential of irisin against diseases involving inflammation, oxidative stress, and apoptosis: An introductory review. Pharmacol Res 2018, 129: 44–55.
71. Batirel S, Bozaykut P, Mutlu Altundag E, Kartal Ozer N, Mantzoros CS. The effect of Irisin on antioxidant system in liver. Free Radic Biol Med 2014, 75(Suppl 1): S16.
72. Lu JY, Xiang GD, Liu M, Mei W, Xiang L, Dong J. Irisin protects against endothelial injury and ameliorates atherosclerosis in apolipoprotein E-Null diabetic mice. Atherosclerosis 2015, 243: 438–448.
73. Pearson-Smith JN, Patel M. Metabolic dysfunction and oxidative stress in epilepsy. Int J Mol Sci 2017, 18: E2365.
74. Elhady M, Youness ER, Gafar HS, Abdel Aziz A, Mostafa RSI. Circulating irisin and chemerin levels as predictors of seizure control in children with idiopathic epilepsy. Neurol Sci 2018, 39: 1453–1458.
75. Asadi Y, Gorjipour F, Behrouzifar S, Vakili A. Irisin peptide protects brain against ischemic injury through reducing apoptosis and enhancing BDNF in a rodent model of stroke. Neurochem Res 2018, 43: 1549–1560.
76. Greenberg ME, Xu BJ, Lu B, Hempstead BL. New insights in the biology of BDNF synthesis and release: Implications in CNS function. J Neurosci 2009, 29: 12764–12767.
77. Wu BW, Wu MS, Guo JD. Effects of microRNA-10a on synapse remodeling in hippocampal neurons and neuronal cell proliferation and apoptosis through the BDNF-TrkB signaling pathway in a rat model of Alzheimer's disease. J Cell Physiol 2018, 233: 5281–5292.
78. Lin TW, Harward SC, Huang YZ, McNamara JO. Targeting BDNF/TrkB pathways for preventing or suppressing epilepsy. Neuropharmacology 2020, 167: 107734.
79. Lu B, Nagappan G, Lu Y. BDNF and synaptic plasticity, cognitive function, and dysfunction. Handb Exp Pharmacol 2014, 220: 223–250.
80. Numakawa T, Suzuki S, Kumamaru E, Adachi N, Richards M, Kunugi H. BDNF function and intracellular signaling in neurons. Histol Histopathol 2010, 25: 237–258.
81. Kang DH, Choi BY, Lee SH, Kho AR, Jeong JH, Hong DK, *et al*. Effects of cerebrolysin on hippocampal neuronal death after pilocarpine-induced seizure. Front Neurosci 2020, 14: 568813.
82. Nieto-Gonzalez JL, Jensen K. BDNF depresses excitability of parvalbumin-positive interneurons through an M-like current in rat dentate gyrus. PLoS One 2013, 8: e67318.
83. Osehobo P, Adams B, Sazgar M, Xu Y, Racine RJ, Fahnestock M. Brain-derived neurotrophic factor infusion delays amygdala and perforant path kindling without affecting paired-pulse measures of neuronal inhibition in adult rats. Neuroscience 1999, 92: 1367–1375.
84. LaFrance WC Jr, Leaver K, Stopa EG, Papandonatos GD, Blum AS. Decreased serum BDNF levels in patients with epileptic and psychogenic nonepileptic seizures. Neurology 2010, 75: 1285–1291.
85. Safari F, Anvari Z, Moshtaghioun S, Javan M, Bayat G, Forosh SS, *et al*. Differential expression of cardiac uncoupling proteins 2 and 3 in response to myocardial ischemia-reperfusion in rats. Life Sci 2014, 98: 68–74.
86. Safari F, Bayat G, Shekarforoush S, Hekmatimoghaddam S, Anvari Z, Moghadam MF, *et al*. Expressional profile of cardiac uncoupling protein-2 following myocardial ischemia reperfusion in losartan- and ramiprilat-treated rats. J Renin Angiotensin Aldosterone Syst 2014, 15: 209–217.
87. Bechmann I, Diano S, Warden CH, Bartfai T, Nitsch R, Horvath TL. Brain mitochondrial uncoupling protein 2 (UCP2): A protective stress signal in neuronal injury. Biochem Pharmacol 2002, 64: 363–367.
88. Guo XP, Zhang MM, Gao Y, Cao GZ, Lu D, Li WJ. Quantitative multi-omics analysis of the effects of mitochondrial dysfunction on lipid metabolism in *Saccharomyces cerevisiae*. Appl Microbiol Biotechnol 2020, 104: 1211–1226.
89. Horvath TL, Diano S, Leranth C, Garcia-Segura LM, Cowley MA, Shanabrough M, *et al*. Coenzyme Q induces nigral mitochondrial

uncoupling and prevents dopamine cell loss in a primate model of Parkinson's disease. Endocrinology 2003, 144: 2757–2760.
90. Gupta RC, Milatovic D, Dettbarn WD. Depletion of energy metabolites following acetylcholinesterase inhibitor-induced status epilepticus: Protection by antioxidants. Neurotoxicology 2001, 22: 271–282.
91. Gupta RC, Milatovic D, Dettbarn WD. Nitric oxide modulates high-energy phosphates in brain regions of rats intoxicated with diisopropylphosphorofluoridate or carbofuran: Prevention by N-tert-butyl-alpha-phenylnitrone or vitamin E. Arch Toxicol 2001, 75: 346–356.
92. Chan SHH, Wu CWJ, Chang AYW, Hsu KS, Chan JYH. Transcriptional upregulation of brain-derived neurotrophic factor in rostral ventrolateral medulla by angiotensin II: Significance in superoxide homeostasis and neural regulation of arterial pressure. Circ Res 2010, 107: 1127–1139.
93. Bumanglag AV, Sloviter RS. No latency to dentate granule cell epileptogenesis in experimental temporal lobe epilepsy with hippocampal sclerosis. Epilepsia 2018, 59: 2019–2034.
94. Wu J, Vogel T, Gao X, Lin B, Kulwin C, Chen JH. Neuroprotective effect of dexmedetomidine in a murine model of traumatic brain injury. Sci Rep 2018, 8: 4935.
95. Tse K, Hammond D, Simpson D, Beynon RJ, Beamer E, Tymianski M, *et al*. The impact of postsynaptic density 95 blocking peptide (Tat-NR2B9c) and an iNOS inhibitor (1400W) on proteomic profile of the hippocampus in C57BL/6J mouse model of kainate-induced epileptogenesis. J Neurosci Res 2019, 97: 1378–1392.
96. Basu J, Zaremba JD, Cheung SK, Hitti FL, Zemelman BV, Losonczy A, *et al*. Gating of hippocampal activity, plasticity, and memory by entorhinal cortex long-range inhibition. Science 2016, 351: aaa5694.
97. Cheng HM, Wang Y, Chen JZ, Chen Z. The piriform cortex in epilepsy: What we learn from the kindling model. Exp Neurol 2020, 324: 113137.
98. Jin Z, Guo PP, Li XY, Ke JJ, Wang YL, Wu HS. Neuroprotective effects of irisin against cerebral ischemia/reperfusion injury via Notch signaling pathway. Biomed Pharmacother 2019, 120: 109452.
99. Chen C, Li H, Ding F, Yang LL, Huang PY, Wang S, *et al*. Alterations in the hippocampal-thalamic pathway underlying secondarily generalized tonic-clonic seizures in mesial temporal lobe epilepsy: A diffusion tensor imaging study. Epilepsia 2019, 60: 121–130.